Characterization of monolithic CMOS pixel sensor chip with ion beams for application in particle computed tomography

G. Tambave [a,*], J. Alme [a], G.G. Barnaföldi [c], R. Barthel [d], A. van den Brink [d], S. Brons [j], M. Chaar [a],
V. Eikeland [a], G. Genov [a], O. Grøttvik [a], H.E.S. Pettersen [b], Z. Pastuovic [k], S. Huiberts [a],
H. Helstrup [e], K.F. Hetland [e], S. Mehendale [a], I. Meric [e], Q.W. Malik [g], O.H. Odland [a,b], G. Papp [f],
T. Peitzmann [d], P. Piersimoni [a], A. Ur Rehman [a], F. Reidt [m], M. Richter [g], D. Röhrich [a], A. Sudar [c,l],
A.T. Samnøy [a], J. Seco [h,i], H. Shafiee [a,e], E.V. Skjæveland [e], J.R. Sølie [a,e], K. Ullaland [a],
M. Varga-Kofarago [l], L. Volz [h,i], B. Wagner [a], S. Yang [a]

[a] Department of Physics and Technology, University of Bergen, 5007 Bergen, Norway
[b] Department of Oncology and Medical Physics, Haukeland University Hospital, 5021 Bergen, Norway
[c] Department for Theoretical Physics, Wigner RCP of the Hungarian Academy of Sciences, 1121 Budapest, Hungary
[d] Institute for Subatomic Physics, Utrecht University/Nikhef, Utrecht, Netherlands
[e] Faculty of Engineering and Science, Western Norway University of Applied Science, 5063 Bergen, Norway
[f] Institute for Physics, Eötvös Loránd University, H-1117, Budapest, Hungary
[g] Department of Physics, University of Oslo, Oslo, Norway
[h] Department of Biomedical Physics in Radiation Oncology, German Cancer Research Center, Heidelberg, Germany
[i] Department of Physics and Astronomy, Heidelberg University, Heidelberg, Germany
[j] Heidelberg Ion Beam Therapy Center (HIT), Heidelberg, Germany
[k] Center for Accelerator Science, ANSTO, Locked bag 2001, Kirrawee DC NSW 2234, Australia
[l] Department of High Energy Physics, Wigner RCP of the Hungarian Academy of Sciences, 1121 Budapest, Hungary
[m] European Organization for Nuclear Research (CERN), Geneva, Switzerland

ARTICLE INFO

ABSTRACT

Particle computed tomography (pCT) is an emerging imaging modality that promises to reduce range uncertainty in particle therapy. The Bergen pCT collaboration aims to develop a novel pCT prototype based on the ALPIDE monolithic CMOS sensor. The planned prototype consist of two tracking planes forming a rear tracker and Digital Tracking Calorimeter (DTC). The DTC will be made of a 41 layer ALPIDE-aluminum sandwich structure. To enable data acquisition at clinical particle rates, a large multiplicity of particles will be measured using the highly-granular ALPIDE sensor. In this work, a first characterization of the ALPIDE sensor performance in ion beams is conducted. Particle hits in the ALPIDE sensor result in charge clusters whose size is related to the chip response and the particle energy deposit. Firstly, measurements in a 10 MeV ^{4}He micro beam have been conducted at the SIRIUS microprobe facility of ANSTO to investigate the dependence of the cluster size on the beam position over the ALPIDE pixel. Here, a variation in cluster size depending on the impinging point of the beam was observed. Additional beam tests were conducted at the Heidelberg Ion-Beam Therapy Center (HIT) investigating the cluster size as a function of the deposited energy by protons and ^{4}He ions in the sensitive volume of the ALPIDE. Results show the expected increase in cluster sizes with deposited energy and a clear difference in cluster sizes for protons and ^{4}He ions. As a conclusion, the variation in cluster size with the impinging point of the beam has to be accounted for to enable accurate energy loss reconstruction with the ALPIDE. This does, however, not affect the tracking of particles through the final prototype, as for that only the center-of-mass of the cluster is relevant.

* Corresponding author.
 E-mail address: Ganesh.Tambave@uib.no (G. Tambave).

1. Introduction

Due to the favorable depth dose profile of charged particles (the Bragg peak), particle therapy, in theory, allows for better sparing of healthy tissue compared to conventional photon therapy. To accurately place the Bragg peak in the tumor, a precise knowledge of the voxelized stopping power of the patient is crucial [1,2]. In current clinical practice, the stopping power is obtained through a conversion from X-ray CT Hounsfield Units (HU) to relative stopping power (RSP), defined as the stopping power of a material relative to that of water. This conversion introduces 2% to 3% (depending on the organ and tissue type) uncertainty in the RSP calculation due to the nonlinear nature of the relation between the Hounsfield Unit and the RSP [3]. In order to ensure accurate treatment, these uncertainties have to be accounted for by including safety margins around the target volume [1,2]. The RSP uncertainties can be improved using the particle computed tomography (pCT) which enables the direct reconstruction of the voxelized RSP [4].

The concept of pCT is imaging with energetic particles (^{1}H, ^{4}He, ^{12}C ions etc.), traversing the object to be reconstructed. The typical prototype pCT scanner consists of thin tracking detectors placed in front of and behind the patient to measure the trajectories of the particles entering and exiting the patient. After the rear tracking detector an energy or a range detector is used to measure the residual energy or range of the particles. The image is reconstructed by rotating the pCT scanner around the patient. There are several attempts being made on developing a prototype pCT scanner [4]. However, so far no clinical system exists.

In this context, the Bergen pCT collaboration is building a prototype pCT scanner based on a monolithic CMOS sensor named ALPIDE [5]. It will be used as a rear tracking detector and in a range detector called Digital Tracking Calorimeter (DTC). The entrance vector at the object will be determined using combination of pencil beam position and the pixel location in the rear tracker [6]. The DTC will host 41 sandwiched layers of ALPIDE (50 μm thick) and Aluminum (3.5 mm thick). There will be 108 ALPIDE chips per layer and the total size of the DTC will be 15×27 cm^2. The design concept of a DTC for pCT has been explored in [7], which also reports that the range of individual proton can be determined with WET (Water Equivalent Thickness) resolution of about 1.2% in a non-degraded beam.

The ALPIDE (ALICE PIxel DEtector) was originally developed for the upgrade of the Inner Tracking System (ITS) of the ALICE experiment at the LHC, CERN [5]. The chip is fabricated on a substrates with a high-resistivity (>1 kΩ cm) epitaxial layer (25 μm thick). The chip measures 15×30 mm^2 and contains a matrix of 512×1024 pixels with in-pixel amplification, shaping, discrimination and multi-event buffering. The pixel size is 29.24×26.88 μm^2 which makes the ALPIDE a highly granular sensor capable of simultaneous tracking of multiple particles. The readout of the pixel matrix implements zero suppression: only the addresses of pixels actually hit are sent off chip which provides efficient tracking at high ion-beam rate. The detector is expected to track about 10 million particles per second. Due to this feature, the pCT scan will probably be completed in few minutes. The reference [5] reports the performance of the ALPIDE for the ALICE ITS case: a spatial resolution of 5 μm and a tracking efficiency of about 100% (both for minimum ionizing particles) and a fake hit probability less than 10^{-5} event^{-1} pixel^{-1}. The above mentioned features make the ALPIDE chip an ideal candidate for a pCT scanner. In this paper, the characterization results of the ALPIDE chip for the pCT application are reported.

2. ALPIDE characterization using ion beams

To test the dependence of the average cluster size on the beam position as well as on the energy-loss of ions in the ALPIDE, ion-beam tests were carried out at the SIRIUS microprobe facility of ANSTO, Australia [8], and at the Heidelberg Ion Beam Therapy Center (HIT) [9], Germany, respectively. The test setup photographs are show in Fig. 1.
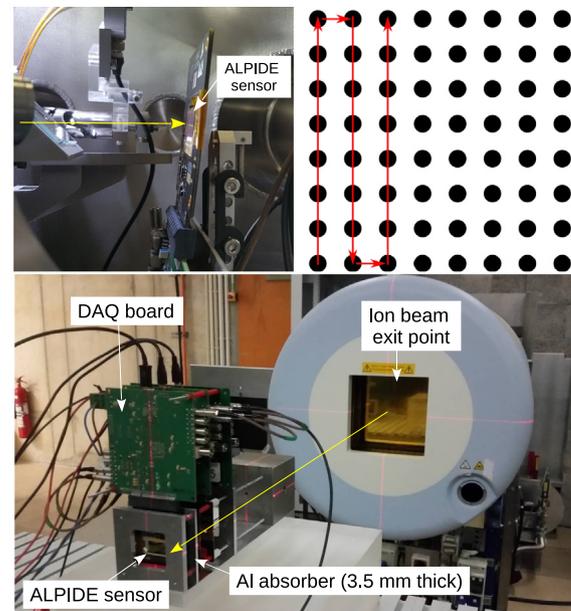

Fig. 1. [Top left] The single ALPIDE chip wire-bonded to a carrier card and coupled to the DAQ board, kept inside the vacuum chamber during the micro beam experiment at the ANSTO facility Australia. [Top right] The drawing shows the pattern of the beam scan. Each dot represents a beam spot and the red arrows show the way the beam spot was scanned across the ALPIDE pixels. [Bottom] Telescope of the three ALPIDE chips each connected to their DAQ boards mounted at the HIT facility, Heidelberg.

2.1. Dependence of the cluster size on the beam position

The microprobe facility test investigates if the cluster size changes with the position where the energy is deposited in the ALPIDE pixel. A group of pixels which are fired by an impinging particle and share a common edge are called a cluster. The count pixels contained in such a cluster is referred to as cluster size. Since the ALPIDE pixels share the same epitaxial layer and there is no insulating barrier between the pixels, they share the charge liberated by a traversing particle. The charge liberated in the pixel is directly proportional to the energy deposited in the silicon. Therefore, the more energy deposited, the higher the charge liberation and this charge will diffuse further and reach more pixels leading to larger clusters. Hence, during this test, the beam used had high LET (Linear Energy Transfer) in the epitaxial layer of the ALPIDE pixel.

The test was conducted using a ^{4}He beam of 10 MeV energy, 10 kHz beam rate, and beam diameter of 1 μm. The ALPIDE chip with its readout board was kept inside the vacuum chamber (see Fig. 1[top left]) and due to space limitations inside the chamber, the chip was tilted by an angle of about 5° with respect to the beam direction. The beam scan-pattern is shown in Fig. 1 [top right]. Here each dot depicts a position of the beam spot and the arrow shows the way the beam spot was scanned over the ALPIDE pixels. The beam was raster scanned over the area of 128×128 μm^2 (4.4×4.8 pixels). The time spent by the beam on each spot was about 200 ms and then moved to the next spot by keeping the distance of 1 μm between each spot.

The ALPIDE carrier card was connected to a data acquisition (DAQ) board equipped with an FPGA and the sampled data was sent to a PC via a USB-3 interface. The ALPIDE pixels latch the hits into their memory when there is a trigger signal and a pixel signal above the discrimination threshold. An external TTL trigger signal generated using a function generator was sent to the ALPIDE via the DAQ board. The trigger rate was kept at 100 kHz (10 μs period) for a burst of 100 triggers, followed by a delay of 100 ms to allow the DAQ board to transfer the data to the computer. The chip was set to integrate over all signals within the 10 μs between two triggers.
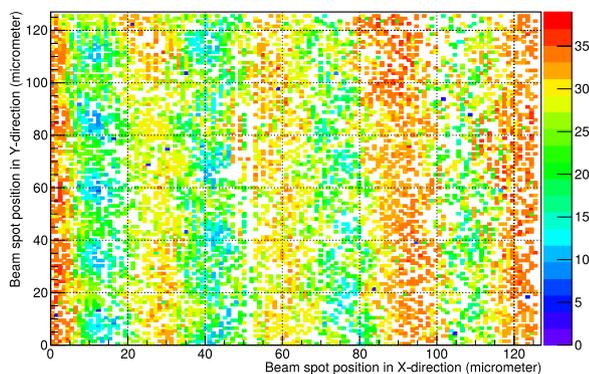
Fig. 2. Average cluster size versus beam position obtained at 0 V back bias. This histogram is for the test done using micrometer size beam to study cluster size dependence on the beam position.
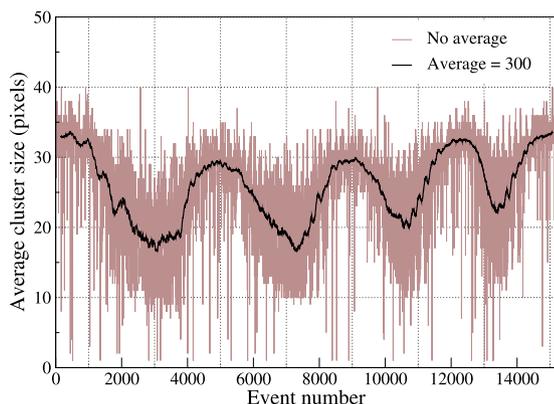

Fig. 3. Average cluster size versus event number. Here the event number is the trigger id for each time frame of about 10 μs. The scan time increases with the increase in the event number while the beam position changed.

The micro-beam test results show that the cluster size changes with the position of the beam as shown in the cluster map in Fig. 2. Here, the cluster size varies as color changes from violet to red as seen on the color axis. During this test the number of pixels scanned was around 4 to 5 in both X-and Y-directions. The scan starts at the bottom left pixel and further moves to a new spot every 200 ms (see Fig. 1 [top right]). The X-and Y-positions plotted in Fig. 2 are obtained by accumulating events for 200 ms and then the average cluster size is calculated for that particular beam position. The cluster map shows that the clusters are rather constant in the vertical-bands visible for various X-positions, but for the various Y-positions the sizes differ in a band structure. It is assumed that the clusters could be smaller when the beam was focused in the close vicinity of the collection node than in the periphery of the node. In the depletion zone close to the collection node, the charge drifts directly to the node and is not shared via diffusion.

The same data sample is shown in a different way by plotting the average cluster size as a function of the event number as shown in Fig. 3. Here, a moving average filtered (size = 300) data is plotted on top of the raw data to highlight the change in the cluster size which follows an oscillation pattern. There are about four peaks in this pattern which correspond to the number of pixels scanned in the *x*-direction. The beam was moved from left to right, changing the beam position across the columns while incrementing the scan time. The visible fluctuation in the clusters could be due to the process variations (some areas of the pixel are slightly more sensitive than the others). Moreover, the ALPIDE was kept in vacuum without cooling so the clusters may fluctuate due to the rise in the temperature of the ALPIDE. The clusters fluctuation with beam position has to be accounted for to
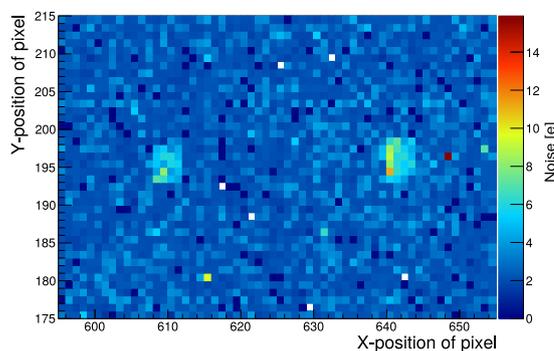

Fig. 4. Noise map of ALPIDE chip zoomed in on the two positions irradiated with ^{4}He ion beam. The noise at these two positions may have increased due to the received dose. The dose delivered to the left spot is about 1.3 kGy and to the right is about 13 kGy. This dose is roughly equivalent to the 1 M pCT scan and 10 M pCT scans, respectively.

enable accurate energy loss reconstruction with the ALPIDE. However, it dose not have any direct impact on the particle tracking for pCT since the center of the cluster is used in the particle tracking.

To study the effect of radiation on the ALPIDE after its prolonged use in the prototype pCT scanner, a very high dose was delivered to a small area (few pixels) of the ALPIDE chip. The effect of the radiation dose is visible in the noise map of the ALPIDE shown in Fig. 4. In this noise map, the two irradiated regions are visible where the noise is higher compared to the non-irradiation pixels of the ALPIDE. The dose delivered to the left spot is about 1.3 kGy and to the right is about 13 kGy. This dose is roughly equivalent to 1 million and 10 million full 3D pCT scans, respectively. This conclusion is based on the calculated average-dose per scan of about 1 mGy for 150 MeV protons given to DTC. Apart from the increased noise no other issues were noticed and the ALPIDE worked fine.

2.2. Dependence of the cluster size on the energy-loss

A new experiment was carried out at the HIT facility in Heidelberg which provides clinical energies for ^{4}He ions and protons. The aim was to study the dependence of the average cluster size on the energy deposited in the ALPIDE chip. A stack of three chips was irradiated with the available He-ion energies of 50, 100.19, 150.11, 200.38 and 220.5 MeV/u and proton energies of 48.12, 200.11, and 221.06 MeV. The beam extraction time was 12 seconds while the beam intensities were about 10^5 particles per second. The aluminum (Al) absorber (3.5 mm thick) was added between layer-2 and layer-3. Each layer was separated by 26 mm and the gap between Al and layer-3 was 6 mm. The settings used for the ALPIDE and for the DAQ were the same as used in the microprobe experiment (see Section 2.1). The EUDAQ and EUTelescope framework [10] adopted for the ALPIDE was used for the data acquisition and data analysis (tracking and the alignment of the detector layers), respectively.

A typical cluster size distribution for protons of 48.2 MeV in the second layer is shown in Fig. 5. The clusters in the distribution are correlated to the proton tracks. The result shows that it is possible to track the protons down to 48.2 MeV energy using the ALPIDE chip. For layer-3, the mean cluster-size versus the energy-loss of the ^{4}He ions and protons with and without an Al absorber is shown in Fig. 6. The energy-loss values are obtained using the stopping power library reported in [11]. Here the standard deviation of the cluster size distribution is used as error bars on the mean cluster size. The proton clusters are smaller compared to the ^{4}He ion clusters, and the clusters produced by both ions vary with the energy-loss. This information is useful while reconstructing the residual range of the ions. The deposited energy (dE/dz) of ion is obtained via the cluster size and depth (z) in the
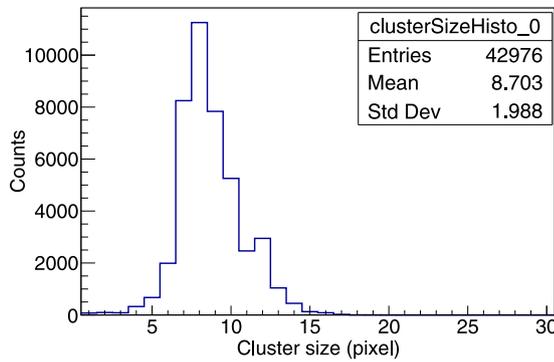
Fig. 5. An example of a typical cluster size distribution for protons of 48.2 MeV (the energy-loss in the ALPIDE is about 0.12 MeV) in the second layer. The clusters are correlated to the proton tracks.
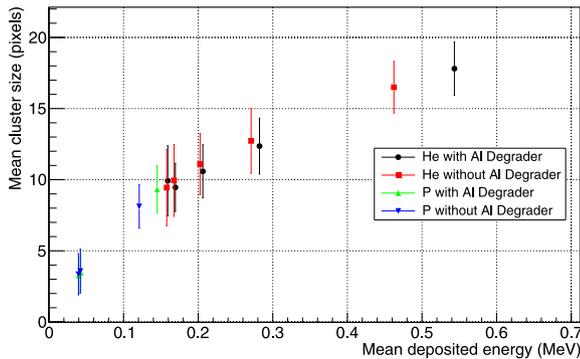

Fig. 6. The mean cluster size versus the energy-loss of the ^{4}He ions and protons in the ALPIDE chip with and without an aluminum absorber (3.5 mm thick) placed in front of layer-3. Here the standard deviation of the cluster size distribution is used as error bars on the mean cluster size. The energy-loss values are obtained using the stopping power library reported in [11].

detector. The fit of Bragg–Kleeman model to the dE/dz data points gives the residual range of the ions with less than 0.2 mm WET systematic error [7].

3. Summary

In this article, two ion-beam test results of the ALPIDE are reported. In the first test, a micrometer size ^{4}He beam was scanned over a few pixels of the ALPIDE. The results show that the cluster size changes with the beam position. However this will not affect the tracking capabilities of ALPIDE since the center of the cluster is used in the particle tracking. In the second test, a stack of three ALPIDE chips was irradiated with ^{4}He ions and protons of various energies. This test showed that the cluster size varies with the increase in the energy-loss of ions in the ALPIDE and it is possible to track protons down to 48.2 MeV energy using the ALPIDE chip. Further work will focus on modeling the cluster size as a function of energy in order to enable energy loss measurements with the ALPIDE chip.

Acknowledgments

References

[1] H. Paganetti, Range uncertainties in proton therapy and the role of MC simulations, Phys. Med. Biol. 57 (11) (2012) R99–R117, http://dx.doi.org/10.1088/0031-9155/57/11/r99.

[2] A.-C. Knopf, In vivoproton range verification: a review, Phys. Med. Biol. 58 (15) (2013) R131–R160, http://dx.doi.org/10.1088/0031-9155/58/15/r131.

[3] B. Schaffner, The precision of proton range calculations in proton radiotherapy treatment planning, Phys. Med. Biol. 43 (6) (1998) 1579–1592, https://www.ncbi.nlm.nih.gov/pubmed/9651027.

[4] R.P. Johnson, Review of medical radiography and tomography with proton beams, Rep. Progr. Phys. 81 (1) (2017) 016701, https://doi.org/10.1088/1361-6633/aa8b1d.

[5] G.A. Rinella, The ALPIDE pixel sensor chip for the upgrade of the ALICE ITS, Nucl. Instrum. Methods A 845 (2017) 583–587, http://dx.doi.org/10.1016/j.nima.2016.05.016.

[6] N. Krah, A comprehensive theoretical comparison of proton imaging set-ups in terms of spatial resolution, Phys. Med. Biol. 63 (2018) 135013, http://dx.doi.org/10.1088/1361-6560/aaca1f.

[7] H. Pettersen, Design optimization of a pixel-based range telescope for proton computed tomography, Phys. Med. Biol. 63 (2019) 87–97, http://dx.doi.org/10.1016/j.ejmp.2019.05.026.

[8] Z. Pastuovic, The new confocal heavy ion microprobe beamline at ANSTO, Nucl. Instrum. Methods A 404 (2017) 1–8, http://dx.doi.org/10.1016/j.nimb.2017.01.059.

[9] S.E. Combs, Particle therapy at the HIT center, Radiother. Oncol. 95 (1) (2010) 41–44, http://dx.doi.org/10.1016/j.radonc.2010.02.016.

[10] M. Varga-Kofarago, (Ph.D. thesis), Utrecht University, 2018, https://dspace.library.uu.nl/handle/1874/360607.

[11] J. Toftegaard, Improvements in the stopping power library libdedx and .., J. Phys. Conf. Ser. 489 (2014) 012003, http://dx.doi.org/10.1088/1742-6596/489/1/012003.